Advances in Brief

Role of Host Microenvironment in Angiogenesis and Microvascular Functions in Human Breast Cancer Xenografts: Mammary Fat Pad *versus* Cranial Tumors[1]

Wayne L. Monsky,[2] Carla Mouta Carreira,[3] Yoshikazu Tsuzuki,[4] Takeshi Gohongi,[5] Dai Fukumura,[6] and Rakesh K. Jain

Edwin L. Steele Laboratory, Department of Radiation Oncology, Massachusetts General Hospital and Harvard Medical School, Boston, Massachusetts 02114

Abstract

Purpose: **The host microenvironment differs between primary and metastatic sites, affecting gene expression and various physiological functions. Here we show the differences in the physiological parameters between orthotopic primary and metastatic breast tumor xenografts using intravital microscopy and reveal the relationship between angiogenic gene expression and microvascular functions *in vivo*.**

Experimental Design: **ZR75-1, a human estrogen-dependent mammary carcinoma, was implanted into the mammary fat pad (primary site) of ovariectomized SCID female mice carrying estrogen pellets. The same tumor line was also grown in the cranial window (metastasis site). When tumors reached the diameter of 2.5 mm, angiogenesis, hemodynamics, and vascular permeability were measured by intravital microscopy, and expression of angiogenic growth factors was determined by quantitative reverse transcription-PCR.**

Results: **ZR75-1 tumors grown in the mammary fat pad had higher microvascular permeability but lower vascular density than the same tumors grown in the cranial window (2.5- and 0.7-fold, respectively). There was no significant difference in RBC velocity, vessel diameter, blood flow rate, and shear rate between two sites. The levels of vascular endothelial growth factor (VEGF), its receptors VEGFR1 and VEGFR2, and angiopoietin-1 mRNA tended to be higher in the mammary fat pad tumors than in the cranial tumors (1.5-, 1.5-, 3-, and 2-fold, respectively).**

Conclusions: **The primary breast cancer exhibited higher vascular permeability, but the cranial tumor showed more angiogenesis, suggesting that the cranial environment is leakage resistant but proangiogenic. Collectively, host microenvironment is an important determinant of tumor gene expression and microvascular functions, and, thus, orthotopic breast tumor models should be useful for obtaining clinically relevant information.**

Introduction

There is a growing body of evidence that the microenvironment in which tumors grow affects their biology, as well as the delivery and efficacy of therapeutic agents (Refs. 1–10; Table 1). Therefore, a quantitative analysis of the effects of the primary and metastatic microenvironment on tumor angiogenesis and microvascular functions, such as hemodynamics, vascular permeability, and growth factor expression, should provide useful insight for cancer treatment. Breast cancer is a leading cause of death in women. A correlation between angiogenesis and prognosis in breast cancer patients has been demonstrated in a number of studies (11, 12). However, to our knowledge, there is no report on the microvascular functional parameters of human breast carcinomas in primary and metastasis sites. To this end, we measured gene expression, angiogenesis, and vascular permeability in a human mammary carcinoma grown orthotopically in the mammary fat pad (primary site) and in a transparent cranial window model (a metastatic site). Various angiogenic factors (VEGF,[7] Ang-1 and 2) and receptors (VEGFR1 and R2) were determined by quantitative RT-PCR. Angiogenesis (microvascular density), hemodynamics (RBC velocity, vessel diameter, blood flow, and shear rate), and vascular permeability were measured using intravital microscopy.

Materials and Methods

Cell Line and Animal Models. ZR75-1 estrogen-dependent human mammary carcinoma cells were grown in DMEM with 10% fetal bovine serum. Female SCID mice (6–8 weeks), weighing ~25 g, were used following institutional guidelines. They were anesthetized by 90 mg of ketamine hydrochloride

Received 10/5/2001; revised 12/5/2001; accepted 12/5/2001.
The costs of publication of this article were defrayed in part by the payment of page charges. This article must therefore be hereby marked *advertisement* in accordance with 18 U.S.C. Section 1734 solely to indicate this fact.
[1] Supported by the U.S. Army Medical Research and Material Command under DAMD 17-98-1-8088 and Program Project Grant PO1-CA80124 from the National Cancer Institute (to D. F. and R. K. J.).
[2] Present address: Department of Radiobiological Sciences, Beth Israel-Deaconess Medical Center, Boston, MA 02115.
[3] Present address: Center for Molecular Medicine, Maine Medical Center Research Institute, Scarborough, ME 04174.
[4] Present address: Department of Internal Medicine II, National Defense Medical College, Saitama 359-8513, Japan.
[5] Present address: Department of Surgery, Tsukuba Gakuen Hospital, Ibaraki 305-8558, Japan.
[6] To whom request for reprints should be addressed, at Department of Radiation Oncology, Massachusetts General Hospital, 100 Blossom Street, Cox-736, Boston MA 02114. Phone: (617) 726-8143; Fax: (617) 724-5841; E-mail: dai@steele.mgh.harvard.edu.

[7] The abbreviations used are: VEGF, vascular endothelial growth factor; RT-PCR, reverse transcription-PCR; CNS, central nervous system; Ang-1, angiopoietin-1.

Table 1 Role of host microenvironment in angiogenesis and vascular functions

Comparison	Reference	Key conclusions
Cranium *vs.* dorsal skin	(2)	Faster angiogenesis in a collagen gel in the cranial window.
	(5)	Smaller pore cut off size in the cranial tumors.
	(6)	Lower vascular permeability in baseline and after VEGF superfusion in pial vessels.
	(8)	Higher interstitial diffusion in the cranial tumors attributable to less collagen (fibroblasts).
	(4)	Tumor blood barrier formation in HGL21 human glioma only when grown in the cranial window.
Liver *vs.* dorsal skin	(3)	Lower VEGF expression and angiogenesis but higher vascular permeability in the liver tumor.
Gall bladder *vs.* s.c.	(7)	Higher production of endogenous antiangiogenesis factor in the orthotopic gall bladder tumor.
Pancreas *vs.* abdominal wall	(9)	Higher VEGF protein level, angiogenesis, and tumor growth in tumors grown in the pancreas.
Cranium *vs.* mammary fat pad	This study	Higher permeability but lower angiogenesis in the mammary fat pad tumor compared with the cranial tumor.

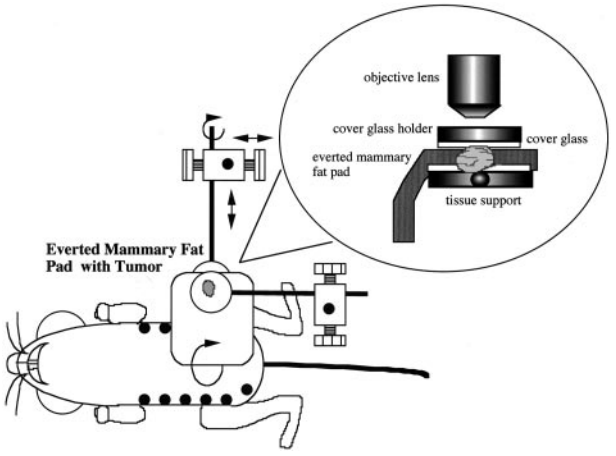

Fig. 1 The mammary fat pad model for microcirculatory and angiogenesis studies. Everted ventral skin flap containing mammary fat pad tissue with implanted tumors was placed on a specialized stage and covered with an 11-mm circular glass coverslip.

and 9 mg of xylazine/kg s.c. Cells (3×10^6; final volume of 30 μl in PBS) were injected using a 30-gauge needle under a dissecting microscope into the mammary fat pad just inferior to the nipple of ovariectomized female SCID mice, while avoiding leakage to s.c. space. Mice were ovariectomized and implanted with control release pellets containing 0.75 mg of estrogen for 60-day release (Innovative Research, Sarasota, FL) 1 week before tumor implantation; this allows enough time to recover from estrogen depletion-induced changes in hemodynamics (13) and avoids the effect of endogenous estrogen, which may vary between animals. For intravital microscopy (under the same anesthetics), a midline incision was made through skin and fascia, and a flap was gently elevated by blunt dissection, not disrupting the vasculature and avoiding irritation of the tumor vessels. The flap with mammary tumor was then placed on a specially designed stage developed originally for the liver preparation (3), and a glass coverslip was placed over the tumor to allow intravital microscopy and analysis of microvascular parameters (Fig. 1). The mouse cranial window model (14) was used to mimic meningeal metastasis. Measurements of microcirculatory parameters were made on tumors grown in both the mammary fat pad and the cranial window when the tumors reached the diameter of ~2.5 mm (~4 weeks after the tumor implantation). Tumor volume doubling times during the exponential growth phase were ~5 and ~8 days for cranial window and mammary fat pad models, respectively.

Measurements of Angiogenesis and Hemodynamics. The experimental procedure for intravital microscopy was described previously (15). Briefly, anesthetized animals were injected i.v. with 100 μl of 10 mg/ml FITC-labeled dextran solution (MW, 2,000,000; Sigma Chemical Co., St. Louis, MO). Epi-illumination was performed using a 100-W mercury lamp equipped with a fluorescence filter for FITC (excitation: 525–555 nm, emission: 580–635 nm). An intensified charge-coupled device video camera (C2400–88; Hamamatsu Photonics K.K., Hamamatsu, Japan) was used to visualize microvessels in five random areas of each tumor. Functional vascular density (an index of angiogenesis) was measured as the total length of perfused vessels per unit area of observation field (16). RBC velocity was measured by the four-slit method (Microflow system, model 208C, videophotometer version; IPM, San Diego, CA; Ref. 16). Vessel diameter was measured by an image-shearing device (digital video image shearing monitor, model 908; IPM; Ref. 16). Mean blood flow rates and shear rates of individual vessels were calculated using vessel diameter and mean RBC velocity as described previously (16).

Microvascular Permeability Measurement. Mice were injected with a bolus (100 μl) of 1% tetramethylrhodamine-labeled BSA (Molecular Probes, Eugene, OR) in saline via the tail vein. Fluorescence intensity of the tumor tissue was measured every 2 min for a total of 20 min by a photomultiplier (9203B; EMI, Rockaway, NJ) in a well-perfused area using a ×20 objective lens. The microvascular permeability to albumin was then calculated as described previously (17).

Preparation of RNA. Tumors were excised, placed on 1.5-ml microcentrifuge tubes, immediately frozen in liquid nitrogen, and stored at −70°C until further analysis. Total RNAs were isolated from each tumor using RNAzol B (Tel-Test, Inc., Friendswood, TX). Slight modifications were introduced to the protocol recommended by the manufacturer to eliminate sample contamination during the homogenization step. Mainly, tumors were turned into a powder with sterile ceramic mortar and pestles cooled with liquid nitrogen and then homogenized to completion in RNAzol B with sterile disposable mini-pellet pestles (Kontes Pellet Pestle) attached to a Cordless Motor (Fisher Scientific, Pittsburgh, PA). The homogenization was done at low temperatures by keeping the microcentrifuge tubes containing the tumor on a metal block precooled for 30 min on

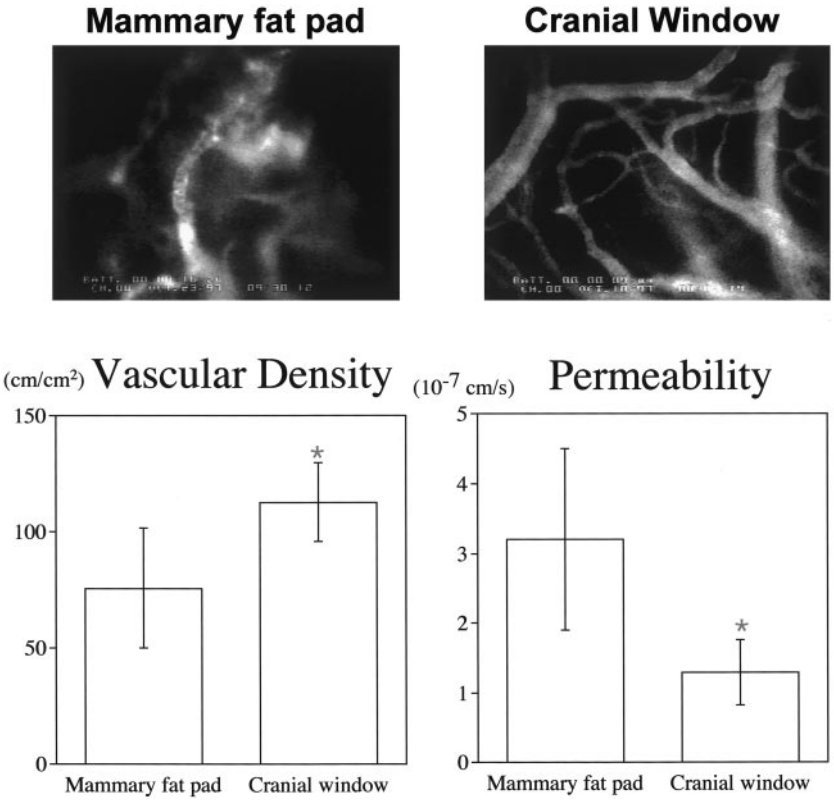

Fig. 2 Microvascular architecture and physiological parameters in ZR75-1 tumors grown in two different sites. *Top row*, representative intravital microscopy images (20 × objective). Blood vessels were contrast enhanced by *i.v.* injection of FITC-dextran. *Bottom left*, vessel density in ZR75-1 tumors grown in two different sites. ZR75-1 tumors grew in either the mammary fat pad or the cranial window microenvironment ($n = 4$ for each site). Five areas per tumor were determined. Vascular density was significantly higher in the cranial tumors as compared with the mammary tumors. *Bottom right*, vascular permeability in ZR75-1 tumors grown in two different sites. Vascular permeability was significantly higher in tumors grown in the mammary fat pad than when grown in the cranial window. Data are expressed as mean ±SD. $*P < 0.05$ as compared with mammary fat pad tumors.

dry ice. For complete removal of DNA contamination, each RNA preparation was treated subsequently with DNase I using the Message Clean system (GenHunter Corp., Nashville, TN). RNAs obtained by this procedure were typically of high quality, as assessed by A260/A280 ratios and by size analysis by denaturing gel electrophoresis using the RNA Millennium marker (Ambion, Inc., Austin, TX). RNAs were stored in aliquots at −70°C at concentrations > 1 μg/ml in diethyl pyrocarbonate-treated water.

Reverse Transcription. RNAs were reverse transcribed into cDNA using the conditions specified in the TaqMan Reverse Transcription Reagents system (PE Applied Biosystems, Foster City, CA). Typically, 1 μg of total RNA was reverse transcribed with oligo $d(T)_{16}$ primers in a final reaction volume of 100 μl.

Quantitative PCR for Angiogenic Growth Factor Expression. Primers followed the requirements specified in the manual for SYBR Green Real Time PCR (PE Applied Biosystems) and were designed on the basis of the known sequences and exon-intron structures (when available) of the mouse and human genes reported in the GenBank and with the help of Primer 3 [Whitehead Institute for Biomedical Research, Steve Rozen, Helen J. Skaletsky (1996, 1997) obtainable as Freeware].[8] Primer sequences were as follows: VEGF-A (FP: 5′-CCT TGC TGC TCT ACC TCC AC-3′; RP: 5′-CAC ACA GGA TGG CTT GAA GA-3′), VEGFR1 (FP: 5′-AAA AAT GGC CAC CAC TCA AG-3′; RP: 5′-GGA GAT CCG AGA GAA AAT GG-3′), VEGFR2 (FP: 5′-GGA GAA GAA TGT GGT TAA GAT CTG TGA-3′; RP: 5′-ACA CAT CGC TCT GAA TTG TGT ATA CTC-3′), Ang-1 (FP: 5′-AGG CTT GGT TTC TCG TCA GA-3′; RP: 5′-TCT GCA CAG TCT CGA AAT GG-3′), HPRT (normalizer for RNA content; FP: 5′- TTA CCA GTG TCA ATT ATA TCT TCA ACA ATC-3′). Primers were synthesized by Integrated DNA Technologies, Inc. (Coralville, IA), and the optimal conditions for their use were determined according to the Taq-Man PCR Reagents protocol. Nontumor human and mouse total RNAs used as positive controls (lung, heart, ovary, liver, and brain) were obtained from Ambion, Inc. RNA samples that had not been reverse transcribed (minus-reverse transcription control) were included in the PCR reactions as negative controls. The size of the PCR products, as well as the presence of a single band, was assessed by electrophoresis of the RT-PCR reactions on NuSieve 3:1 agarose gels (FMC Bioproducts, Rockland, ME) and comparison with several DNA ladders (PCR Marker 50–2000 bp; Parfect DNA 100-bp ladder, Novagen, Madison, WI). Quantification of each cDNA was done relatively to calibrator samples (mouse heart), after the exact instructions from the manufacturer (PE Applied Biosystems).

Statistical Analysis. Data were expressed as mean ± SD. The difference between mammary tumors and cranial tumors was analyzed by Mann-Whitney *U* test. $P < 0.05$ was considered to be statistically significant.

[8] Internet address: http://www-genome.wi.mit.edu/cgi-bin/primer/primer3.cgi.

Table 2 Hemodynamics in ZR75-1 tumors grown in two different sites[a]

Implantation site	RBC velocity (μm/s)	Vessel diameter (μm)	Flow rate (pl/s)	Shear rate (1/s)
Mammary fat pad	189 ± 16	24.4 ± 5.0	111 ± 64	74 ± 10
Cranial window	206 ± 41	23.9 ± 6.8	104 ± 43	89 ± 24

[a] There was no statistically significant difference between two sites. Twenty regions in four tumors were evaluated for each site.

Table 3 Expression of angiogenic growth factors/receptors[a]

Implantation site	hVEGF[b]	VEGFR1	VEGFR2	Ang-1
Mammary fat pad	34 ± 23	5.3 ± 1.5	0.9 ± 0.3[c]	0.9 ± 0.3[c]
Cranial window	22 ± 9	3.6 ± 1.7	0.3 ± 0.2	0.4 ± 0.1

[a] Gene expression levels relative to *HPRT* gene (control) expression are presented. Three tumors were evaluated for each site.
[b] Human VEGF.
[c] $P < 0.05$ as compared with cranial window data.

Results

Angiogenesis in Breast Cancer. Fig. 2 shows representative images of tumor vasculature in ZR75-1 tumors grown either in the mammary fat pad or the cranial window. Tumor vessels are tortuous and irregular. The mammary fat pad tumor exhibited relatively poor vascularity, and the vessels had more irregular shape compared with the cranial tumor vessels. We quantified vessel density and vessel diameter as measures of angiogenesis by intravital microscopy and subsequent image analysis (14). Mammary carcinomas grown in the mammary fat pad had a lower vascular density than tumors grown in the cranial window (76 ± 26 cm/cm^2; 113 ± 17 cm/cm^2; $P = 0.02$; Fig. 2) and comparable vessel diameter (Table 2). Thus, the cranial ZR75-1 tumors (metastasis site) had a higher/larger blood vessel volume than the same tumor grown in mammary fat pad (primary site).

Hemodynamics in Breast Cancer. Blood flow in the tumor vessels was slow and sluggish regardless of implantation site. No significant difference was found between the mammary fat pad tumor and the cranial window tumor in hemodynamics in individual vessels, including RBC velocity, vessel diameter, blood flow, and shear rate in tumors (Table.1). Hemodynamics and angiogenesis data collectively show that cranial tumors have greater blood perfusion than mammary fat pad tumors.

Vascular Permeability in Breast Cancer. Vascular hyperpermeability is a hallmark of tumor vessels. ZR75-1 tumors grown in the mammary fat pad had a significantly higher vascular permeability than tumors grown in the cranial window ($3.2 \pm 1.3 \times 10^{-7}$ cm/s; $1.3 \pm 0.5 \times 10^{-7}$ cm/s; $P = 0.04$; Fig. 2).

Angiogenic Factor Expression in Breast Cancer. To gain mechanistic insight into the vascular phenotype of ZR75-1 tumors grown in different sites, we determined angiogenic factor/receptor expression by quantitative RT-PCR. VEGFR2 (Flk-1) and Ang-1 mRNA expression in the mammary fat pad tumors were statistically significantly higher than those in the cranial tumors (Table 3). VEGF and VEGFR1 (flt-1) also tended to be higher in the mammary tumors. Ang-2 expression was not detectable in either site in the conditions used.

Discussion

We developed a novel method to study tumor angiogenesis and microcirculation at primary and metastatic sites for a human mammary carcinoma. Although both spontaneous (transgenic) and xenografted tumors in the mammary fat pad have been used extensively in breast cancer research (18–20), there is still a paucity of data on microvascular functions in orthotopic breast tumors. Mouse and rat dorsal skin chambers are used frequently to study physiological functions in tumors (21, 22). However, the take rate of human breast tumor xenografts, such as ZR75-1 and MCF-7, is usually low in the dorsal skin chamber. In fact, the mammary fat pad has been shown to be a more favorable graft site for the mammary cancer because of its good blood supply in contrast to the skin site (23). Our present report shows that ZR75-1 tumors could also grow well in the cranial window model, which constitutes an orthotopic environment for leptomeningeal metastasis. Metastasis of mammary carcinoma to the CNS and leptomeninges is less common than to bone, lung, or liver (24, 25). However, CNS involvement is refractory to treatment (26), and thus, it is important to understand the differences in tumor microenvironment that may contribute to this treatment resistance.

Using these two breast cancer models, we found that breast cancer grown in different sites has different angiogenic gene expression and microvascular characteristics. VEGF is one of the most potent angiogenic and vascular permeability factors. It is expressed in most human malignant tumors. VEGF has been shown to increase angiogenesis, tumor growth, and experimental metastasis in breast cancer (27). Angiopoietins play important roles in a later phase of developmental angiogenesis, such as remodeling and maturation of vessel network. Ang-1 induces angiogenesis and reduces vascular permeability in the skin vessels (28). Receptors to VEGF and Angs, such as Flt-1/Flk-1 and Tie-2, respectively, are predominantly expressed on vascular endothelial cells. VEGF is known to induce its receptors' expression. Our quantitative RT-PCR data showed that both VEGF and Ang-1, as well as VEGF receptors, tend to be expressed at a higher level in tumors grown in the mammary fat pad (primary site) than in the cranial window (metastasis site). Increased expression of VEGF, VEGF receptors, Flt-1, and Flk-1 has also been reported in breast cancer tissue from patients (29). However, vascular density in the mammary fat pad tumors is lower than in the cranial tumors. This is counterintuitive and suggests that we should be cautious about predicting functional outcome of different organ sites simply from the concentration of putative growth factors. We have shown previously that angiogenesis in collagen gels containing known concentrations of VEGF or basic fibroblast growth factor is significantly faster in the cranial window than in the dorsal skin chamber (2). Thus, higher vessel density and blood flow rate underlying pial tissue may potentiate the angiogenic response to tumor factors. In addition, the response of host vascular endothelial cells to the stimuli, or the recruitment of circulating endothelial cells, may be host organ dependent. Finally, other angiogenic or antian-

giogenic factors may also be involved. Tissue level of mRNA should be interpreted carefully as well. Protein level expression and/or localization is more relevant to the functional outcome.

Contrary to the vascular density (angiogenesis), vascular permeability was significantly higher in tumors grown in the mammary fat pad than those grown in the cranial window. Higher VEGFR2 expression in the mammary tumors may explain, in part, the increased permeability. However, Ang-1 was also higher in the mammary tumors, but it was 40 times lower than VEGF. Although Ang-1 is known to induce resistance to leakiness in the skin vessels, this may not be the case for the tumor vessels. Blood vessels in the CNS are known to have tight junctions and form blood brain barrier. Tumors in the brain also show similar selectivity in vascular permeability (30). We reported previously that vessels of tumors grown in cranial windows are less permeable to albumin and exhibit smaller pore size compared with tumors grown in s.c. space (4–6, 14). Furthermore, vascular permeability change in response to VEGF is much lower in pial vessels compared with that in s.c. vessels (6). Collectively, vessels in the cranial environment or those originating from endothelial cells with tight junctions exhibit less leakiness to macromolecules.

To summarize, vascular permeability in the primary breast cancer was higher than that in the brain metastasis. On the other hand, cranial tumors showed more angiogenesis. These data suggest that cranial environment is leakage resistant but proangiogenic. Collectively, the present study underscores the importance of the host microenvironment in gene expression and physiological functions and suggests that the orthotopic breast tumor models be used to obtain clinically relevant information.

Acknowledgments

We thank Drs. Claus Kristensen and Fan Yuan for their helpful input, and Dr. Yi Chen, Ms. Julia Kahn, and Sylvie Roberge for their excellent technical assistance.

References

1. Fidler, I. J. Modulation of the organ microenvironment for treatment of cancer metastasis. J. Natl. Cancer Inst. (Bethesda), *87:* 1588–1592, 1995.

2. Dellian, M., Witwer, B. P., Salehi, H. A., Yuan, F., and Jain, R. K. Quantitation and physiological characterization of angiogenic vessels in mice: effect of basic fibroblast growth factor, vascular endothelial growth factor/vascular permeability factor, and host microenvironment. Am. J. Pathol., *149:* 59–72, 1996.

3. Fukumura, D., Yuan, F., Monsky, W. L., Chen, Y., and Jain, R. K. Effect of host microenvironment on the microcirculation of human colon adenocarcinoma. Am. J. Pathol., *151:* 679–688, 1997.

4. Jain, R. K. The Eugene M. Landis Award Lecture. Delivery of molecular and cellular medicine to solid tumors. Microcirculation, *4:* 1–23, 1997.

5. Hobbs, S. K., Monsky, W. L., Yuan, F., Roberts, G., Griffith, L., Torchillin, V., and Jain, R. K. Regulation of transport pathways in tumor vessels: role of tumor type and host microenvironment. Proc. Natl. Acad. Sci. USA, *95:* 4607–4612, 1998.

6. Monsky, W. L., Fukumura, D., Gohongi, T., Ancukiewcz, M., Weich, H. A., Torchilin, V. P., Yuan, F., and Jain, R. K. Augmentation of transvascular transport of macromolecules and nanoparticles in tumors using vascular endothelial growth factor. Cancer Res., *59:* 4129–4135, 1999.

7. Gohongi, T., Fukumura, D., Boucher, Y., Yun, C-O., Soff, G. A., Compton, C., Todoroki, T., and Jain, R. K. Tumor-host interactions in the gallbladder suppress distal angiogenesis and tumor growth: involvement of transforming growth factor β1. Nat. Med., *5:* 1203–1208, 1999.

8. Pluen, A., Boucher, Y., Ramanujan, S., McKee, T. D., Gohongi, T., diTomasso, E., Brown, E. B., Izumi, Y., Campbell, R. B., Berk, D. A., and Jain, R. K. Role of tumor-host interactions in interstitial diffusion of macromolecules: cranial *vs.* subcutaneous tumors. Proc. Natl. Acad. Sci. USA, *98:* 4628–4633, 2001.

9. Tsuzuki, Y., Carreira, C. M., Bockhorn, M., Xu, L., Jain, R. K., and Fukumura, D. Pancreas microenvironment promotes VEGF expression and tumor growth: novel window models for pancreatic tumor angiogenesis and microcirculation. Lab. Investig., *81:* 1439–1452, 2001.

10. Fidler, I. J. Angiogenic heterogenity: regulation of neoplastic angiogenesis by the organ microenvironment. J. Natl. Cancer Inst. (Bethesda), *93:* 1040–1041, 2001.

11. Kumar, S., Ghellal, A., Li, C., Byrne, G., Haboubi, N., Wang, J. M., and Bundred, N. Breast carcinoma: vascular density determined using CD105 antibody correlates with tumor prognosis. Cancer Res., *59:* 856–861, 1999.

12. Folkman, J. Tumor angiogenesis. *In:* J. F. Holand, E. I. Frei, R. C. J. Bast, D. W. Kufe, P. E. Pollock, and R. R. Weichselbauum (eds.), Cancer Medicine, Ed. 5, pp. 132–152. Ontario: B.C. Decker, Inc., 2000.

13. Kristensen, C. A., Hamberg, L. M., Hunter, G. J., Roberge, S., Kierstead, D., Wolf, G. L., and Jain, R. K. Changes in vascularization of human breast cancer xenografts responding to antiestrogen therapy. Neoplasia, *1:* 1–9, 1999.

14. Yuan, F., Salehi, H. A., Boucher, Y., Vasthare, U. S., Tuma, R. F., and Jain, R. K. Vascular permeability and microcirculation of gliomas and mammary carcinomas transplanted in rat and mouse cranial window. Cancer Res., *54:* 4564–4568, 1994.

15. Yuan, F., Leunig, M., Berk, D. A., and Jain, R. K. Microvascular permeability of albumin, vascular surface area, and vascular volume measured in human adenocarcinoma LS174T using dorsal chamber in SCID mice. Microvasc. Res., *45:* 269–289, 1993.

16. Leunig, M., Yuan, F., Menger, M. D., Boucher, Y., Goetz, A. E., Messmer, K., and Jain, R. K. Angiogenesis, microvascular architecture, microhemodynamics, and interstitial fluid pressure during early growth of human adenocarcinoma LS174T in SCID mice. Cancer Res., *52:* 6553–6560, 1992.

17. Yuan, F., Chen, Y., Dellian, M., Safabakhsh, N., Ferrara, N., and Jain, R. K. Time-dependent vascular regression and permeability changes in established human tumor xenografts induced by an anti-vascular endothelial growth factor/vascular permeability factor antibody. Proc. Natl. Acad. Sci. USA, *93:* 14765–14770, 1996.

18. Xiao, G., Liu, Y. E., Gents, R., Sang, Q. A., NI, J., Goldberg, I. D., and Shi, Y. E. Suppression of breast cancer growth and metastasis by a seprin myoepithelium-derived serine proteinase inhibitor expressed in the mammary myoepithelial cells. Proc. Natl. Acad. Sci. USA, *96:* 3700–3705, 1999.

19. Hutchinson, J. N., and Muller, W. J. Transgenic mouse models of human breast cancer. Oncogene, *19:* 6130–6137, 2000.

20. Chatzistamou, L., Schally, A. V., Nagy, A., Armatis, P., Szepeshazi, K., and Halmos, G. Effective treatment of metastatic MDA-MB-435 human estrogen-independent breast carcinomas with a targeted cytotoxic analogue of luteinizing hormone-releasing hormone NA-207. Clin. Cancer Res., *6:* 4158–4165, 2000.

21. Jain, R. K., Munn, L. L., and Fukumura, D. Transparent window models and intravital microscopy. *In:* B. A. Teicher (ed.), Tumor Models in Cancer Research, pp. 647–671. Totowa: Humana Press, Inc., 2001.

22. Dewhirst, M. W., Tso, C. Y., Oliver, R., Gustafson, C. S., Secomb, T. W., and Gross, J. F. Morphologic and hemodynamic comparison of tumor and healing normal tissue microvasculature. Int. J. Radiat. Oncol. Biol. Phys., *17:* 91–99, 1989.

23. Price, J. E., Polzos, A., Zhang, R. D., and Daniels, L. M. Tumirigenecity and metastasis of human breast carcinoma cell lines in nude mice. Cancer Res., *50:* 717–721, 1990.

24. Olson, M. E., Chernik, N. L., and Posner, J. B. Infiltration of the leptomeninges by systemic cancer. A clinical and pathologic study. Arch. Neurol., *30:* 122–137, 1974.

25. Zinser, J. W., Hortobagyi, G. N., Buzdar, A. U., Smith, T. L., and Fraschini, G. Clinical course of breast cancer patients with liver metastases. J. Clin. Oncol., *5:* 773–782, 1987.

26. Olson, M. E., Chernik, N. L., and Posner, J. B. Leptomeningeal metastasis from systemic cancer: a report of 47 cases. Trans. Am. Neurol. Assoc., *96:* 291–293, 1971.

27. Zhang, H. T., Craft, P., Scott, P. A., Ziche, M., Weich, H. A., Harris, A. L., and Bicknell, R. Enhancement of tumor growth and vascular density by transfection of vascular endothelial growth factor into MCF-7 human breast carcinoma cells. J. Natl. Cancer Inst. (Bethesda), *87:* 213–219, 1995.

28. Thurston, G., Suri, C., Smith, K., McClain, J., Sato, T. N., Yancopoulos, G. D., and McDonald, D. M. Leakage-resistant blood vessels in mice transgenically overexpressing angiopoietin-1. Science (Wash. DC), *286:* 2511–2514, 1999.

29. Brown, L. F., Guidi, A. J., Schnitt, S. J., Van De Water, L., Iruela-Arispe, M. L., Yeo, T. K., Tognazzi, K., and Dvorak, H. F. Vascular stroma formation in carcinoma *in situ*, invasive carcinoma, and metastatic carcinoma of the breast. Clin. Cancer Res., *5:* 1041–1056, 1999.

30. Roberts, W. G., Delaat, J., Nagane, M., Huang, S., Cavenee, W. K., and Palade, G. E. Host microvasculature influence on tumor vascular morphology and endothelial gene expression. Am. J. Pathol., *153:* 1239–1248, 1998.

Clinical Cancer Research

Role of Host Microenvironment in Angiogenesis and Microvascular Functions in Human Breast Cancer Xenografts: Mammary Fat Pad *versus* Cranial Tumors

Wayne L. Monsky, Carla Mouta Carreira, Yoshikazu Tsuzuki, et al.

Clin Cancer Res 2002;8:1008-1013.